

A Numerical Analysis of Initiation of Polymerization Waves

A. HEIFETZ

Department of Electrical and Computer Engineering
Northwestern University, Evanston, IL 60208-3118, U.S.A.

L. R. RITTER

Department of Mathematics
Texas A&M University, College Station, TX 77843-3368, U.S.A.

W. E. OLMSTEAD AND V. A. VOLPERT

Department of Engineering, Science, and Applied Mathematics,
Northwestern University, Evanston, IL 60208-3125, U.S.A.

(Received August 2003; revised and accepted November 2003)

Abstract—Frontal polymerization is a process of converting a monomer into a polymer by means of a self-propagating, thermal reaction wave. We study initiation of polymerization waves by a heat source. A five-species reaction model is considered with a focus on the evolution of two of these species and the temperature of the mixture. We conduct independent numerical analyses of two experimental configurations. The first of these consists of a mixture of monomer and initiator (a catalytic agent) placed in a test tube and a constant high temperature imposed at one end of the tube. Here, we identify four parameters whose values are determined by the rate of initiator decomposition, amount of volumetric heat loss, amount of heat produced by chemical conversion, and initial mixture temperature. We present a marginal initiation criterion as a relation between these parameters. The second experimental configuration considered here involves placing a test tube filled with a monomer and initiator mixture into a hot thermostatic oil bath. Asakur *et al.* recently reported that they had observed the formation of a reaction front in the center of a mixture under these conditions. We offer a simple mathematical model of this experiment and the results of numerical simulations based on this model. We show that the model proposed here captures a phenomenon observed in experiment, namely, that for a given bath temperature, there is a minimal tube radius necessary for a reaction front to be initiated. Our results further confirm that the frontal polymerization observed in such experiments can occur via a thermal mechanism. © 2004 Elsevier Science Ltd. All rights reserved.

Keywords—Frontal polymerization, Initiation, Reaction front.

1. INTRODUCTION

Thermal frontal polymerization is a process of converting a monomer into a polymer by means of a self-propagating, high-temperature reaction wave. The chemical process is usually free-radical polymerization which initially involves two species: a monomer and an initiator, which is needed to start the growth of polymer chains. In a typical experiment, the species are placed in a test tube, and the temperature of the mixture is increased by applying a heat source. The increase

This work was supported in part by the National Science Foundation under Grant DMS-0103856.

in temperature induces decomposition of the initiator which produces active radicals, and the polymer chain growth process begins. Then, chemical conversion occurs in a narrow, localized region. The polymer chain growth occurring in this reaction zone is highly exothermic, and the resulting heat release promotes initiator decomposition ahead of the front. In this way, a self-sustained reaction wave can form. This wave travels through the unreacted mixture leaving polymer in its wake.

Self-propagating reaction waves were first discovered by Merzhanov, Borovinskaya, and Shkiri in 1967 in the context of combustion problems. Their experiments consisted of compressing a powdered mixture of elements into a pellet and igniting the pellet at one end. This resulted in the formation of a reaction front which traveled through the mixture in a self-propagating mode. This process, called *self-propagating high-temperature synthesis*, was used to produce technologically useful ceramic and intermetallic materials [1]. This approach to free-radical polymerization was introduced by Chechilo *et al.* in 1972 [2]. They discovered *frontal polymerization* using vinyl monomers. Chechilo *et al.* conducted several studies of the character of the polymerization process under varying experimental conditions [3–5]. Their results were confirmed by other groups in the Soviet Union during the early 1970s, and there have since been a few other Russian studies of frontal polymerization [6–9]. Experimental studies were resumed in the United States by Pojman during the 1990s. Pojman and others observed polymerization fronts using methacrylic acid [10], undiluted liquid monomer [11,12], and solid monomer [13]. In frontal polymerization, the production of polymer is both rapid and uniform. Continued study of the phenomenon is motivated by the expected benefits over traditional polymerization techniques, namely lower energy cost, reduced waste production, and increased control of product features and quality [14]. For a concise review of thermal frontal polymerization including a history, descriptions of experimental conditions, and observed modes of frontal polymerization, the interested reader is directed to [15]. In [16,17], a mathematical model for a five-species reaction is presented, and traveling wave solutions are sought. In these theoretical examinations of the process, the focus has been on the propagation of the thermal front and its velocity, the spatial profiles of the species involved, the degree of conversion of monomer, and the final temperature of the mixture. Initiation of a polymerization front is presumed. From experimental work, however, it is found that initiation of the front does not always occur. Initiation of frontal polymerization waves by an induced heat flux was examined in [18]. In [18], Ritter *et al.* derive a criterion for initiation of polymerization waves as a two parameter integral equation that admits both singular and global solutions depending on the parameter values. These two types of solutions are interpreted as indicating initiation and noninitiation of a reaction front, respectively. The focus of this paper is on initiation of polymerization waves under different experimental conditions. In particular, we assume that the externally imposed heat source corresponds to subjecting the mixture to a fixed high temperature. The type of analysis used in [18] is not applicable under these conditions. Here, we conduct a numerical study of initiation of polymerization waves. A description of the numerical methods employed is given at the end of Section 2. In this paper, we present independent studies of two types of experiments in free-radical frontal polymerization. For each system, we determine a criterion for initiation of a reaction wave and examine the dependence of this criterion on the various factors of the experiment that tend to promote or inhibit front formation. In particular, we consider the effects of reactant consumption, the amount of heat released by reaction, heat losses to the environment, the initial temperature of the mixture, and the nature of the imposed heat source where appropriate. The focus of Section 2 is a mathematical formulation of a generic experiment in thermal free-radical frontal polymerization. This will include a derivation of the equations of interest and a nondimensionalization of these equations.

Section 3 is devoted to a consideration of an experiment in which a mixture of monomer and initiator is placed into a test tube and a fixed high temperature is imposed at one end of the tube. In the nondimensional formulation of the corresponding equations, we identify four parameters whose values influence whether a reaction front is observed. The values of these

parameters, D , α , δ , and θ_0 , are determined by the rate at which initiator decomposes, the amount of heat lost to the environment, the amount of heat released during chemical conversion, and the initial temperature of the mixture, respectively. A critical condition necessary for a reaction front to be observed is determined as a relationship between these parameters.

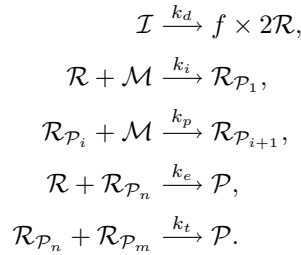
In Section 4, we examine the recently reported phenomenon of the formation of a reaction front at the center of a cylindrical tube and the subsequent propagation of the front radially outwards toward the walls of the tube. In [19], Asakura *et al.* attempted to induce a polymerization front in a test tube filled with monomer and initiator by immersing the tube in a hot thermostatic oil bath. They reported the spontaneous initiation of a front at the center of the test tube in some, but not all, of their experiments. These experimentalists noted that whether a front formed or not depended on bath temperature and the radius of the test tube. Included in Section 4 is a simple mathematical model of this experimental set up. We perform a numerical analysis based on this model, with particular attention to the role of the bath temperature and the radius of the test tube used. Through examinations of the spatial profiles of the system temperature and a reaction term we seek a critical relationship (separating an initiation from a noninitiation regime) between bath temperature and tube radius. Moreover, we confirm that frontal polymerization under these experimental conditions can occur via a thermal mechanism.

2. THE MATHEMATICAL MODEL

The typical experiment in free-radical frontal polymerization involves a mixture of initiator and monomer placed into a test tube. Assuming that the cross sectional area of the tube is small relative to the its length, we can model the tube as a thin channel $0 \leq \hat{x} \leq X$. The following mathematical model for a five-species reaction is proposed in [16,17].

Free-radical frontal polymerization involves a five-step chemical process:

1. the initiator decomposes to produce primary radicals (decomposition),
2. a primary radical can combine with a monomer molecule to produce a polymer radical (chain initiation),
3. the polymer chain propagates as a polymer radical combines with a monomer molecule to produce an additional polymer radical (chain propagation),
4. the final polymer is produced when a polymer radical combines with a free-radical (primary radical termination), or
5. with another polymer radical (polymer radical termination): this process is shown schematically below



The five species are the initiator, primary radicals, monomer, polymer radicals, and the polymer denoted by $\mathcal{I}, \mathcal{R}, \mathcal{M}, \mathcal{R}_{\mathcal{P}}$, and \mathcal{P} , respectively. The notation $\mathcal{R}_{\mathcal{P}_i}$ indicates a polymer radical consisting of i monomer molecules. The term f in the first reaction is the *efficiency factor* and is defined as the ratio of primary radicals in the polymer to the primary radicals formed by the initiator. The reaction rates denoted as k with a subscript are assumed to have an Arrhenius dependence on the temperature of the system. This will be explained shortly.

Letting $\mathcal{I}, \mathcal{R}, \mathcal{M}, \mathcal{R}_{\mathcal{P}}$, and \mathcal{P} , denote the concentrations of initiator, primary radicals, monomer, polymer radicals, and the polymer in dimensional quantities, the following system of equations

governing the kinetics at the time \hat{t} can be written,

$$\frac{dI}{\hat{t}} = -k_d I, \quad (1)$$

$$\frac{dR}{\hat{t}} = 2fk_d I - k_i R M - k_e R R_p, \quad (2)$$

$$\frac{dM}{\hat{t}} = -k_i R M - k_p M R_p, \quad (3)$$

$$\frac{dR_p}{\hat{t}} = k_i R M - k_e R R_p - 2k_t R_p^2, \quad (4)$$

$$\frac{dP}{\hat{t}} = k_e R R_p + k_t R_p^2. \quad (5)$$

In practice, the value of f in the second equation is taken to be 1/2 [16]. The Arrhenius reaction rates can be expressed as

$$k_\alpha(T) = k_\alpha^0 \exp\left(\frac{-E_\alpha}{R_g T}\right), \quad \text{for } \alpha = d, i, p, e, t.$$

Here, k_α^0 is the frequency factor, E_α is the activation energy for the corresponding reaction, and R_g is the universal gas constant. The subscripts correspond to the five reaction steps—initiator decomposition d , polymer chain initiation i , chain propagation p , free radical termination e , and polymer radical termination t .

A formulation of the heat balance in the system is required. Each of the four chemical reactions subsequent to initiator decomposition is exothermic, and the decomposition of initiator is often endothermic but may also occur exothermically. However, it has been determined that the most significant heat release occurs in the propagation step [4]. Only this contribution to the net energy of the system will be considered here. Letting $T(\hat{t}, \hat{x})$ denote the temperature of the mixture at time \hat{t} and at the point \hat{x} , we can write the following reaction-diffusion equation governing the temperature,

$$\frac{\partial T}{\partial \hat{t}} = \kappa \frac{\partial^2 T}{\partial \hat{x}^2} - q \frac{\partial M}{\partial \hat{t}} - \hat{\alpha} (T - T_0).$$

In this formulation, $\kappa > 0$ is the thermal diffusivity of the mixture, $q > 0$ is the heat released per unit reacted monomer, $\alpha \geq 0$ is the volumetric heat loss parameter, and T_0 is the ambient temperature.

When supplemented by the appropriate initial and boundary conditions, equations (1)–(6) govern the state of the experimental mixture. We will consider a reduced system of equations obtained by imposing the quasisteady-state assumption (QSSA) [17], reducing the number of unknowns as in [16,17], and considering only the evolution of the initiator, the monomer, and the temperature. The QSSA states that the level of free and polymer radicals in the mixture is nearly constant. Hence, we put $\frac{d}{d\hat{t}}(R + R_p) = 0$. In addition, we make the simplifying assumptions as justified in [17],

$$k_i = k_p, \quad k_e = k_t, \quad \text{and} \quad R_p \gg R.$$

Summing equations (2),(4) and making the aforementioned assumptions yields

$$R + R_p \approx \sqrt{\frac{2fk_d}{k_t}} \sqrt{I}.$$

Then, (3) becomes

$$\frac{dM}{d\hat{t}} = -k_p \sqrt{\frac{2fk_d}{k_t}} M \sqrt{I}.$$

Noting that the coefficient in front of M in the above equation is an Arrhenius exponential motivates the following convenient notation for the effective reaction rate

$$k_{\text{eff}} = k_p \sqrt{\frac{2fk_d}{k_t}}, \quad k_{\text{eff}}^0 = k_p^0 \sqrt{\frac{2fk_d^0}{k_t^0}}, \quad \text{and} \quad E_{\text{eff}} = \frac{1}{2}(E_d - E_t) + E_p.$$

The initial amounts of monomer and initiator present are known and will be denoted by M_0 and I_0 . Similarly, the initial temperature of the system is given as T_0 . The boundary conditions to be assumed in this paper will change according to the experimental set up under consideration, and will be discussed in the corresponding sections. The reduced dimensional system to be studied can now be stated,

$$\frac{\partial I}{\partial \hat{t}} = -k_d(T) I, \quad I(0) = I_0, \quad (7)$$

$$\frac{\partial M}{\partial \hat{t}} = -k_{\text{eff}}(T) M \sqrt{I}, \quad M(0) = M_0, \quad (8)$$

$$\frac{\partial T}{\partial \hat{t}} = \kappa \frac{\partial^2 T}{\partial \hat{x}^2} + qk_{\text{eff}}(T) M \sqrt{I} - \hat{\alpha}(T - T_0), \quad T(0, \hat{x}) = T_0 \quad \hat{x} \geq 0. \quad (9)$$

2.1. Nondimensionalization

The analysis of the system (7)–(9) is facilitated by introducing a convenient nondimensionalization. To this end, we introduce the nondimensional parameters

$$r = \frac{E_d}{E_{\text{eff}}}, \quad \beta = \frac{R_g T_s}{E_{\text{eff}}}, \quad \delta = \frac{R_g T_s^2}{q M_0 E_{\text{eff}}},$$

$$t_* = \frac{e^{1/\beta}}{k_{\text{eff}}^0}, \quad x_* = \sqrt{\kappa t_*}, \quad \alpha = \hat{\alpha} t_*,$$

and define the nondimensional variables

$$J = \sqrt{\frac{I}{I_0}}, \quad \Psi = \frac{M_0 - M}{M_0}, \quad \theta = \frac{T - T_s}{\beta T_s},$$

$$\theta_0 = \frac{T_0 - T_s}{\beta T_s}, \quad t = \hat{t}/t_*, \quad \text{and} \quad x = \hat{x}/x_*.$$

The term T_s is a scaling temperature. The definition of this scaling temperature will be made precise in the following sections, as our choice of T_s will depend on the type of experimental set up under consideration.

Upon substitution of these variables, we obtain the nondimensional system corresponding to (7)–(9),

$$\frac{\partial J}{\partial t} = -D J \exp\left(\frac{r\theta}{1 + \beta\theta}\right), \quad J(0, x) = 1, \quad (10)$$

$$\frac{\partial \Psi}{\partial t} = (1 - \Psi) J \exp\left(\frac{\theta}{1 + \beta\theta}\right), \quad \Psi(0, x) = 0, \quad (11)$$

$$\frac{\partial \theta}{\partial t} = \frac{\partial^2 \theta}{\partial x^2} + \frac{1}{\delta} (1 - \Psi) J \exp\left(\frac{\theta}{1 + \beta\theta}\right) - \alpha (\theta - \theta_0), \quad \theta(0, x) = \theta_0. \quad (12)$$

The additional parameter D appearing in (10) is defined by

$$D = \frac{k_d(T_s)}{2k_{\text{eff}}(T_s)}.$$

This parameter will be of interest because its magnitude indicates the rate at which initiator decomposes during the polymerization process. If D is very large, we expect that a propagating reaction front would not be observed since the initiator necessary for the reaction to be induced would immediately be depleted. Again, the appropriate boundary conditions depend on the experimental conditions and will be provided in the corresponding sections.

2.2. Numerical Methods

The numerical examinations were performed by using the method of lines. In particular, we chose an equally spaced discretization of the spatial variable— $x_i = i\Delta x$, for $i = 0, 1, \dots, K$ —and assumed that each of the variables $J(t, x)$, $\Psi(t, x)$, and $\theta(t, x)$, are well approximated by an interpolation at the points x_i . We let $J_i(t) = J(t, x_i)$, $\Psi_i(t) = \Psi(t, x_i)$, and $\theta_i(t) = \theta(t, x_i)$, and used a central difference approximation formula for the spatial derivative,

$$\left. \frac{\partial^2 \theta}{\partial x^2} \right|_{x=x_i} \approx \frac{\theta_{i+1}(t) - 2\theta_i(t) + \theta_{i-1}(t)}{\Delta x^2}, \quad \text{for } i = 1, \dots, K-1.$$

At the point of the tube in contact with the external heat source, we set

$$\frac{\partial \theta}{\partial t} = 0.$$

Together with equations (10)–(12), these assumptions define a $3K + 3$ system of ordinary differential equations for the J_i , Ψ_i , and θ_i . This system was solved using the LSODA differential equation solver by Petzold and Hindmarsh. This package automatically switches between stiff and nonstiff methods of solution at each time step so as to minimize computational time while preserving accuracy. The parameter values used for the various computations presented here are chosen to be consistent with typical experimental values. Extensive tabulated values of kinetic parameters (e.g. pre-exponential factors, activation energies, etc.) can be found in [21].

3. INITIATION BY A CONSTANT TEMPERATURE HEAT SOURCE

First, we consider an experiment in which the heat source imposed is a fixed constant temperature T_w at the wall of the test tube ($x = 0$). We chose as a scaling temperature for this problem the wall temperature $T_s = T_w$. The result of this choice is that the boundary condition at $x = 0$ is

$$\theta(t, 0) = 0.$$

We will assume that T_w is large as compared to a typical room temperature, so that by the definition of the initial temperature, we have $\theta_0 < 0$.

Since the length of the test tube is typically very large relative to the width of the reaction zone, we can consider the equations to be given on a semi-infinite line $x \geq 0$. Moreover, the temperature in the far field, that is, as $x \rightarrow \infty$, is unaffected by the reaction, and we can assume the boundary condition,

$$\left. \frac{\partial \theta}{\partial x} \right|_{x \rightarrow \infty} = 0.$$

This no-flux condition in the far field means that we set $\frac{\partial}{\partial x} \theta(t, x_K) = 0$, and at the imposed right-end point (necessary for computation), we use the approximation,

$$\left. \frac{\partial^2 \theta}{\partial x^2} \right|_{x=x_K} \approx \frac{2\theta_{K-1}(t) - 2\theta_K(t)}{\Delta x^2}.$$

The focus of our study is on four experimental factors that tend to promote or inhibit formation and propagation of a reaction front. These correspond to the parameters D , δ , α , and θ_0 , whose values are determined by the rate at which initiator decomposes, the amount of heat produced by the reaction, the amount of heat lost to the environment, and the initial temperature of the system, respectively. For each numerical computation, the value of $D \in (0, 6)$ was fixed and α was varied until a critical value $\alpha_c(D)$ was found, such that, for $\alpha < \alpha_c(D)$, a traveling wave solution was observed, but, for $\alpha > \alpha_c(D)$, either front formation is not observed or the front is

seen to be dampened before wave propagation can begin. Figures 1 and 2 show these observed phenomena (front formation and propagation or failure of a front to form) for selected values of D . An unambiguous change in the qualitative behavior of the temperature profile is seen as α is varied near the critical value. The curve obtained by the pairs $(D, \alpha_c(D))$ represents a marginal initiation curve for the system. The nature of this curve is also dependent on the values of δ and θ_0 .

The adiabatic temperature defined by $T_a = T_0 + qM_0$ is the total increase in temperature due to complete conversion of monomer. Defining the nondimensional adiabatic temperature in the natural way,

$$\theta_a = \frac{T_a - T_s}{\beta T_s},$$

we find that the parameter $\delta^{-1} = \theta_a - \theta_0$. Hence, δ^{-1} represents the (nondimensional) adiabatic temperature increase attainable during an experiment. For fixed β , θ_0 , and M_0 an increase (decrease) in δ^{-1} corresponds to an increase (decrease) in the value of q , which we recall is the amount of heat released per unit reacted monomer. Thus, we expect that a decrease in the value of δ would result in a larger portion of the parameter space (D, α) corresponding to the initiation regime. In Figure 3, the marginal initiation curves for three values of δ are shown. For each value of δ , the region lying below the corresponding curve is the set of (D, α) that will lead to initiation of a polymerization front. As anticipated, this region is increased by taking smaller values of δ . The points that lie above a given curve correspond to the noninitiation regime in which heat lost to the environment (or excessive depletion of initiator) inhibits the formation of a reaction front.

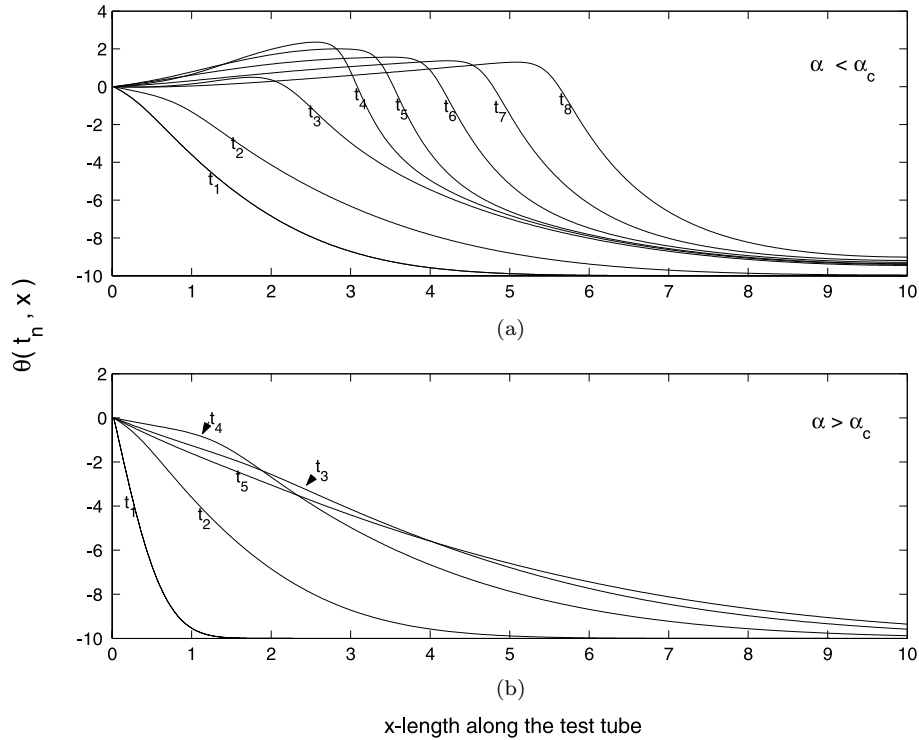


Figure 1. Initiation and noninitiation phenomena for $D = 0.5$. In (a), $\alpha = 0.044$ just below the critical value $\alpha_c(0.5) = 0.0443$, and the formation and propagation of a reaction wave is observed. In (b), $\alpha = 0.045$ and a reaction front does not form. The parameter values of $\theta_0 = -10$, $\beta = 0.09$, $\delta = 0.05$, and $r = 2$ were used for both plots. The times for plot (a) are $t_1 = 1.96$, $t_2 = 5.38$, $t_3 = 11.2$, $t_4 = 11.7$, $t_5 = 11.9$, $t_6 = 12.5$, $t_7 = 13.2$, and $t_8 = 14.1$. The times in plot (b) are $t_1 = 0.121$, $t_2 = 1.96$, $t_3 = 8.46$, $t_4 = 13.5$, and $t_5 = 17.1$.

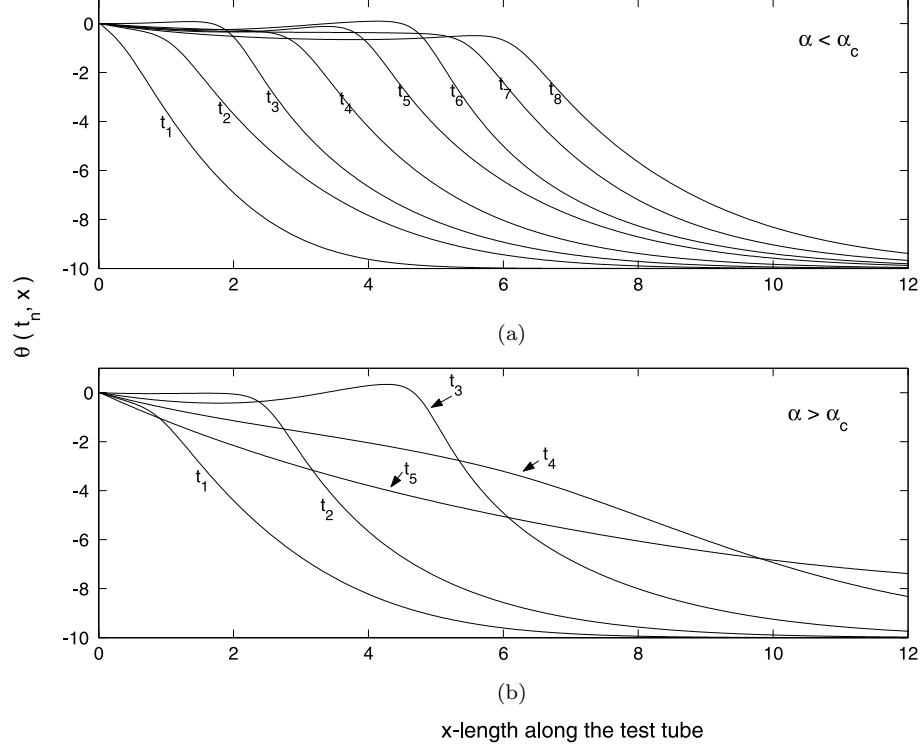


Figure 2. Initiation and noninitiation phenomena for $D = 3.0$ with $\alpha < \alpha_c$ (a) and $\alpha > \alpha_c$ (b). The parameter values used in both plots are $\theta_0 = -10$, $\beta = 0.09$, $\delta = 0.04$, $r = 2$, and in (a) $\alpha = 0.017$ and in (b) $\alpha = 0.020$. The critical value is $\alpha_c(3.0) = 0.018$ for the choice of θ_0 and δ . The times at which the temperature profiles are taken are: (a) $t_1 = 1.83$, $t_2 = 4.87$, $t_3 = 6.63$, $t_4 = 8.71$, $t_5 = 11.3$, $t_6 = 12.6$, $t_7 = 14.4$, $t_8 = 16.6$; (b) $t_1 = 4.23$, $t_2 = 7.73$, $t_3 = 13.8$, $t_4 = 23.2$, $t_5 = 40.1$.

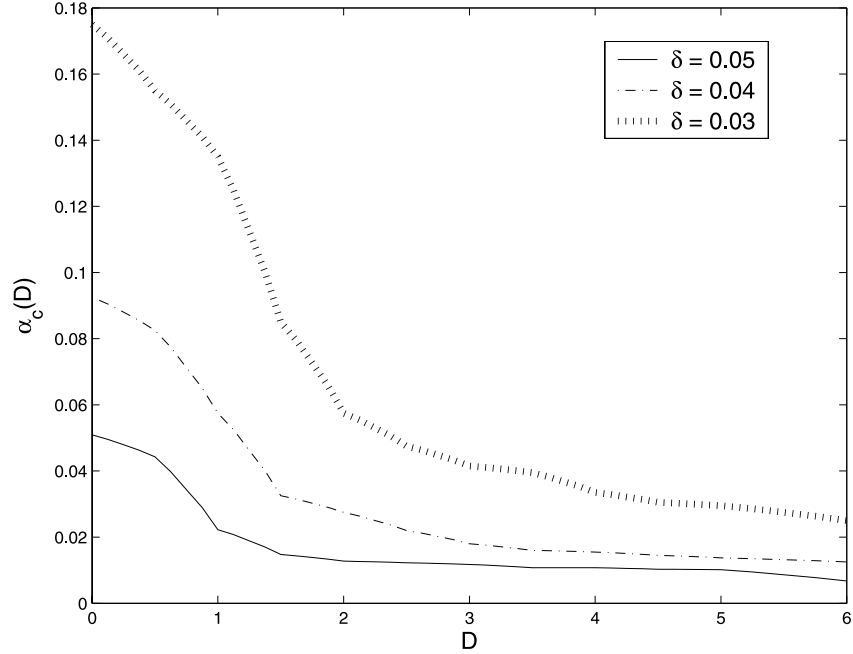


Figure 3. Comparison of marginal initiation curves $(D, \alpha_c(D))$ for various values of δ . For each value of δ , the region lying under the corresponding curve represents the pairs (D, α) that lead to initiation of a polymerization wave. Here, $\beta = 0.09$, $\theta_0 = -10$, and $r = 2$.

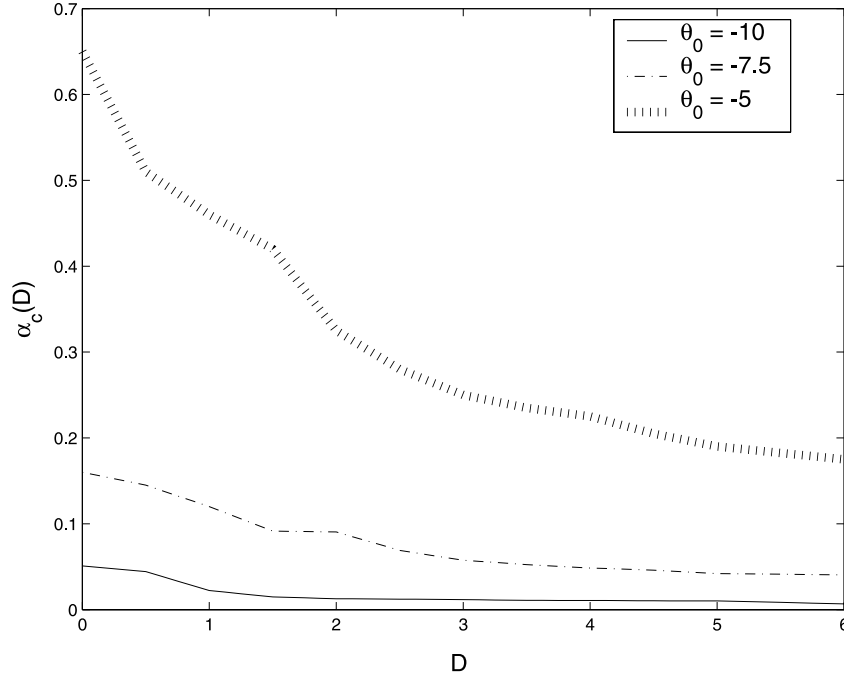


Figure 4. Comparison of marginal initiation curves $(D, \alpha_c(D))$ for various values of θ_0 . For each value of θ_0 the region lying under the corresponding curve represents the pairs (D, α) that lead to initiation of a polymerization wave. Here, $\beta = 0.09$, $\delta = 0.05$, and $r = 2$.

A similar analysis can be made with respect to the initial temperature. For fixed values of β , T_s , δ , and M_0 an increase (decrease) in θ_0 corresponds to a proportional increase (decrease) of the initial temperature in the original, dimensional coordinates. An increase in the initial energy of the system would be expected to result in a larger portion of the parameter space (D, α) corresponding to an initiation regime. That is, for fixed D , a reaction front is attainable even with greater heat losses to the surrounding environment. In Figure 4, this is confirmed. Figure 4 shows the marginal initiation curves for three values of θ_0 keeping β and δ fixed. As in Figure 3, for each curve the regions below and above the curve correspond to the initiation and noninitiation regimes, respectively. Given known (dimensional) values of various kinetic and other parameters (e.g., initial concentrations), it is possible to ensure a reaction wave will form during an experiment by imposing the appropriate temperature at the wall.

4. POLYMERIZATION BY A RADIALLY PROPAGATING FRONT

In this section, we will examine a phenomenon that has been reported by Asakura *et al.* [19], namely, the spontaneous formation of a polymerization front in the center of a cylindrical tube and the ensuing propagation of this front radially outward toward the walls of the tube. Asakura and coworkers intended to produce poly (methyl methacrylate) by immersing a tube of methyl methacrylate and initiator in a thermostatic oil bath. As discussed in this paper, free-radical frontal polymerization by a thermal mechanism is typically initiated in a neighborhood of an imposed external heat source as a direct result of contact with this heat source. Hence, they expected to induce a reaction front at the walls of the tube that would propagate into the interior of the mixture. All of their attempts to induce a polymerization front at the walls of the tube using the oil bath at moderate temperature as a heat source failed. However, they did observe the spontaneous formation of a front at the center of the mixture. This front then propagated radially outward to form the desired polymer. Whether a front formed or not depended on various factors including the temperature of the surrounding bath and the diameter of the test

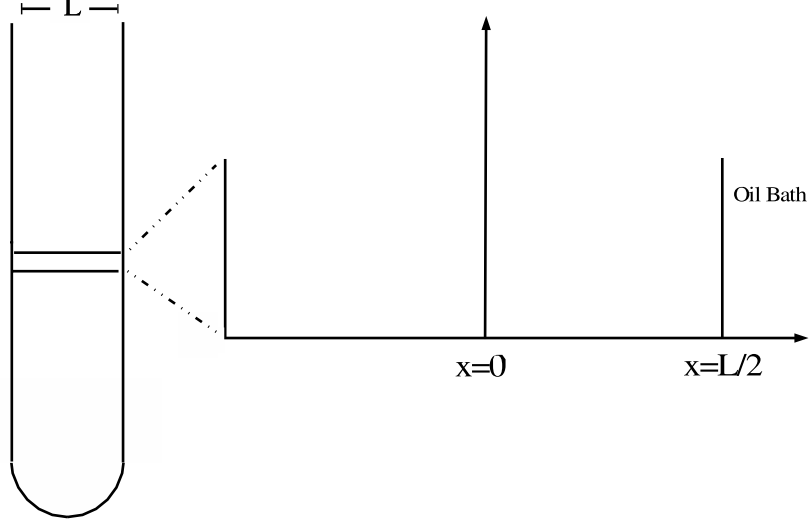


Figure 5. Small section of a test tube showing the imposed coordinate system. Assuming that the behavior of the system, in regards to front formation, is symmetric with respect to $x = 0$, the governing equations are solved on the interval $0 \leq x \leq L/2$ where L is the diameter of the test tube. The temperature is kept at the constant bath temperature at the end $x = L/2$.

tube. These experimentalists recorded observing a critical tube diameter at which the behavior of the reaction changed. The chemical conversion occurred more “abruptly” in larger test tubes [19].

In this section, we present a mathematical model of the spontaneous front formation described above and offer the results of numerical computations based on this model with special attention given to the effects of bath temperature and tube radius. Because we want to account for different values of the bath temperature, it is not desirable to use this as a scaling temperature. For this problem, we will use the adiabatic temperature as defined in Section 3 as our scaling temperature—i.e., $T_s = T_a$. Since this is the total increase in temperature due to reaction, this will mean that all relevant bath temperatures θ_b will satisfy $\theta_b < 0$.

We begin by considering a thin cross-section of the test tube taken perpendicular to its length as depicted in Figure 5. We impose a radial coordinate x as the distance from the center of the test tube $x = 0$ and assume that the behavior of the system is smooth and symmetric with respect to the axis $x = 0$. This symmetry assumption implies a no-flux boundary condition on the temperature at $x = 0$. The wall of the tube is at $x = L/2$ where L is the diameter of the test tube. Here, the system is in contact with the thermostatic oil bath. Hence, we impose the boundary condition on the temperature θ of the mixture $\theta(t, L/2) = \theta_b$, the bath temperature. Since the mixture is immersed in this bath, the initial temperature is also equal to the bath temperature, and we can assume that there is no appreciable volumetric heat loss ($\alpha = 0$). Assuming a planar geometry and that spatial variations occur only in the x -direction, the governing equations are the same as (10)–(12), but the boundary conditions are as just described. The system can be written as

$$\frac{\partial J}{\partial t} = -DJ \exp\left(\frac{r\theta}{1+\beta\theta}\right), \quad J(0, x) = 1, \quad (13)$$

$$\frac{\partial \Psi}{\partial t} = (1 - \Psi) J \exp\left(\frac{\theta}{1+\beta\theta}\right), \quad \Psi(0, x) = 0, \quad (14)$$

$$\frac{\partial \theta}{\partial t} = \frac{\partial^2 \theta}{\partial x^2} + \frac{1}{\delta} (1 - \Psi) J \exp\left(\frac{\theta}{1+\beta\theta}\right), \quad \theta(0, x) = \theta_b, \quad (15)$$

$$\frac{\partial \theta}{\partial x}(t, 0) = 0 \quad \text{and} \quad \theta\left(t, \frac{L}{2}\right) = \theta_b. \quad (16)$$

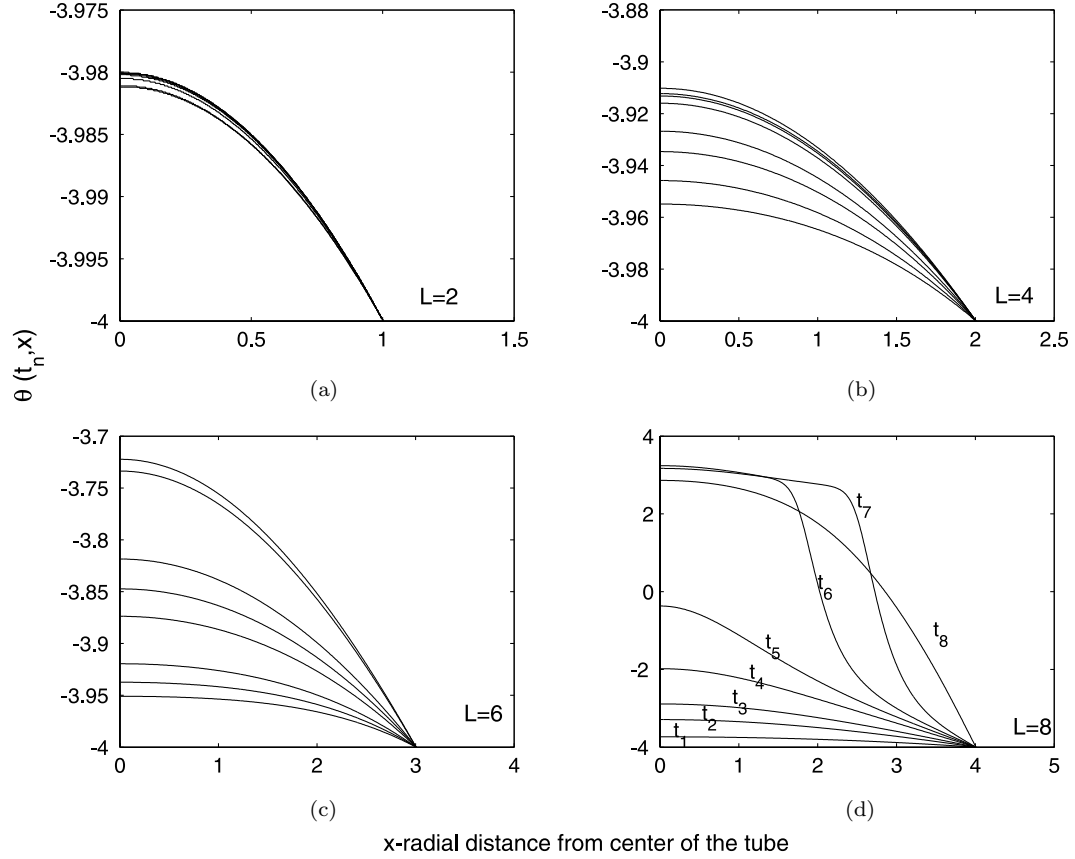


Figure 6. Temperature profiles for fixed bath temperature and four different tube radii. The tubes are of diameter (a) $L = 2$, (b) $L = 4$, (c) $L = 6$, and (d) $L = 8$. Only in (d) where the diameter of the tube is the largest is there a clear formation and propagation of a reaction wave (note the scaling on the temperature axes). For each of these plots, the parameter values $\theta_b = -4$, $\delta = 0.05$, $\beta = 0.09$, and $r = 2$ were taken. The spatial profiles for (a), (b), and (c) are shown at the approximate times $t = 0.3$, $t = 1.4$, $t = 1.8$, $t = 2$, $t = 3$, $t = 5$, $t = 6$, $t = 15$, and $t = 27$. The profiles in (d) are given at the times $t_1 = 0.03$, $t_2 = 6.49$, $t_3 = 16.4$, $t_4 = 20.7$, $t_5 = 23.3$, $t_6 = 24.4$, $t_7 = 24.6$, and $t_8 = 26.0$.

The system (13)–(16) was solved numerically for different values of the bath temperature and the tube radius. Considering a fixed bath temperature, we found that a polymerization front forms (or fails to form) based on the size of the test tube. In Figure 6, spatial temperature profiles at selected times are shown for a fixed bath temperature and four different choices of the tube diameter. We see that for a (nondimensional) tube radius less than some critical value, a front fails to form. The oil bath is intended as a heat source, but its presence has different effects at various stages of the experiment. This bath, while having a high temperature as compared with normal room temperatures (Asakura *et al.* used bath temperatures of 45°C to 60°C), has a temperature that is lower than an expected reaction temperature. During the initial stages of the experiment the temperature in the mixture increases due to contact with the oil bath. A build up of heat in the interior of the mixture eventually acts as a catalyst causing initiator to decompose so that initiation takes place. The temperature increase due to polymer chain growth (when it occurs) results in a mixture temperature that is much higher than the surrounding bath which at this stage of the experiment serves as a heat sink. As evidenced by Figure 6, thermally induced frontal polymerization under these experimental conditions thus requires the test tube be sufficiently large so as to decrease the mixture contact with the heat sink. Figure 7 shows the spatial profile of the reaction term, $\delta^{-1} \frac{\partial \Psi}{\partial t}$, at selected times for the case when a polymerization front forms in the system. A traveling wave solution is seen.

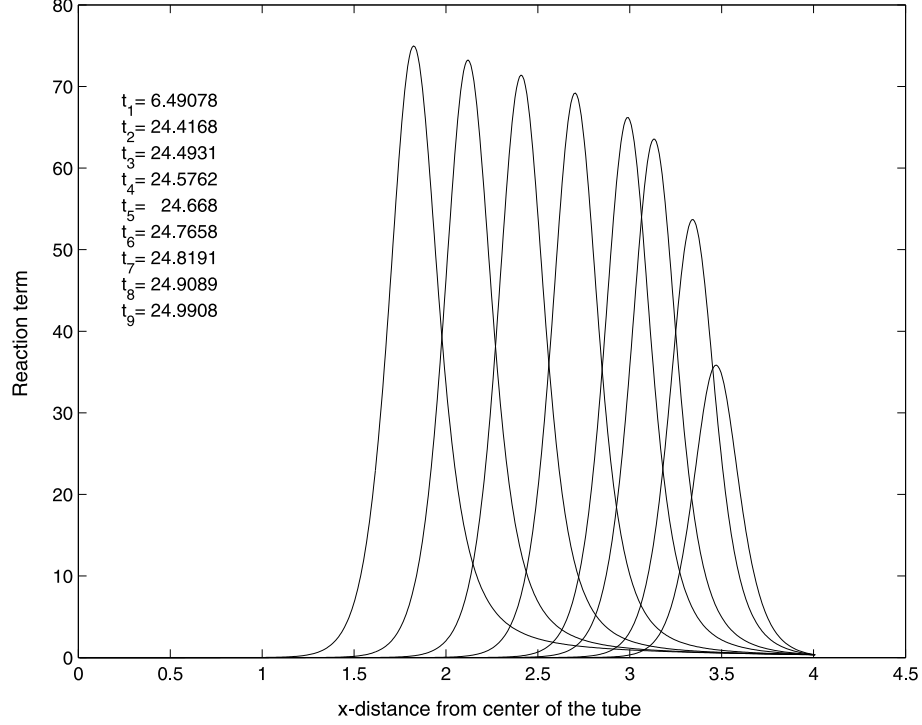


Figure 7. Spatial profile of the reaction term $\delta^{-1} \frac{\partial \Psi}{\partial t}$ at several different times. The profiles correspond to the times shown, t_1 – t_8 from left to right. The point $x = 4$ marks the wall of the test tube in contact with the oil bath. All parameter values are the same as in Figure 6d. A clear propagating reaction is seen.

The numerical computations failed to yield a precise “critical radius” because an intermediate behavior—poorly defined front formation—is observed for values of the radius between those that result in an obvious front and those that clearly result in no front formation whatsoever. Table 1 shows lower and upper bounds on such a critical radius for various values of the bath temperature. Figure 8 shows the change in behavior of both the spatial temperature and reaction term profiles for radii above and below the range of values as shown in Table 1.

We have confirmed through this numerical analysis the finding of Asakura *et al.* It is evident that use of a thermostatic bath as an imposed heat source can induce thermal, radially propagating, frontal polymerization. However, when initiation does occur, it does not do so in a neighborhood of the heat source but rather in the interior of the mixture after sufficient heat build up. If a front does form, then, the temperature of the bath is small relative to the reaction temperature meaning that the bath then acts as a heat sink. For this reason, the test tube used must be sufficiently large in diameter to decrease contact of the mixture with the heat sink and insure front formation and propagation.

Table 1. Bounds on the critical radius needed for thermal front formation.

| Bath Temp. θ_b | Critical Radius (r_c) | |
|--------------------------|---------------------------|-------------|
| | Lower Bound | Upper Bound |
| −1 | 0.30 | 1.00 |
| −2 | 0.73 | 1.00 |
| −3 | 1.25 | 2.00 |
| −4 | 3.50 | 4.00 |

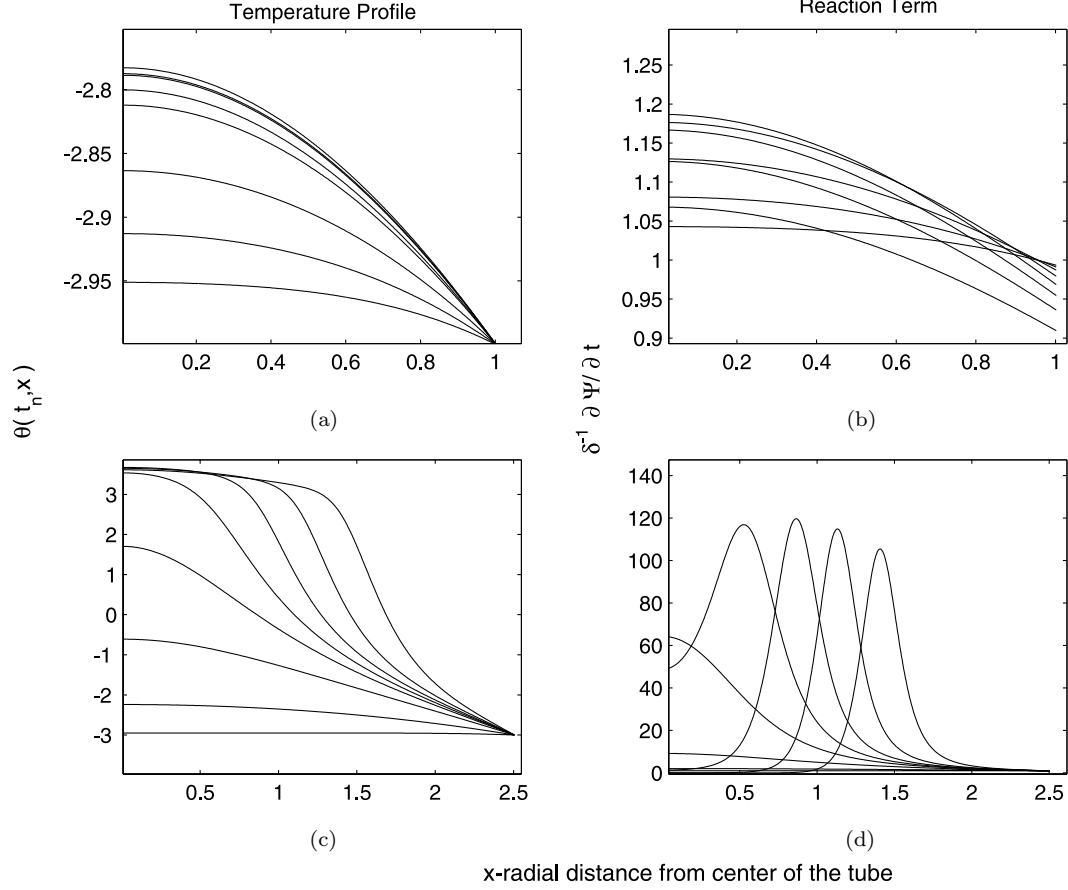


Figure 8. Initiation and noninitiation for bath temperature $\theta_b = -3.0$. (a) and (c) show the spatial temperature profiles for several times $0 < t < 6$ for radii below ($L = 1$) and above ($L = 2.5$), respectively, the value necessary for front formation. The reaction term profiles for the same radii are shown in (b) and (d). (d) shows an unambiguous traveling wave solution.

5. CONCLUSIONS

One goal of any experiment in free-radical frontal polymerization is to induce the formation of a reaction front that will travel through a mixture of monomer and initiator converting it into a polymer. Only after a reaction front forms can various aspects (front velocity, degree of conversion of monomer, etc.) be examined. Insufficient heat put into the system, inadequate amounts of reactants, and heat lost to the environment are some factors that can inhibit reaction front formation. In this paper, we have considered thermal frontal polymerization processes given two different types of experimental set ups. Using appropriate mathematical models, we have attempted, for each of these types of experiments, to derive a criterion based on the conditions of the experiment that will allow us to predict when a reaction front will form.

First, we considered a typical experiment in free-radical frontal polymerization in which the high temperature heat source imposed corresponds to a fixed temperature at the end of the tube. We accounted for reactant depletion and volumetric heat losses. A numerical study of this system was performed as we sought an initiation criterion as a relationship between the parameters governing the state of the mixture. We considered a parameter D that describes the rate of consumption of initiator (the larger the value of D , which is a nonnegative parameter, the faster the initiator is consumed), and a parameter α (also nonnegative) which is determined by the rate at which heat is lost to the environment. Through a series of numerical computations, we were able to determine a critical value $\alpha_c(D)$, such that, for each fixed D $\alpha < \alpha_c$ gave rise

to front formation and propagation while $\alpha > \alpha_c$ resulted in failure of a front to form. The pairs $(D, \alpha_c(D))$ define a marginal initiation curve for the system. The behavior of this curve was then studied as we varied other parameters governing the system, in particular the initial temperature of the mixture and the adiabatic increase in temperature. We found that increasing the initial temperature or the adiabatic increase in temperature resulted in a larger portion of the parameter space (D, α) corresponding to formation and propagation of a reaction front. Our analysis does not account, however, for the role of initial initiator concentration, a factor that was found in [18] to influence front formation under the experimental conditions considered therein. This limitation results from the definitions of the nondimensional variables used here.

Finally, we examined a phenomenon recently reported by Asakura *et al.* in [19]. Asakura and coworkers attempted to produce reaction waves at the walls of a test tube filled with a monomer and initiator mixture by immersing the tube in a hot, thermostatic oil bath. While they were not successful in inducing reaction at the tube walls, they reported observing the spontaneous formation of a front at the center of the tube. Then, this front propagated radially outward toward the tube walls. By considering a thin cross-section of the test tube and assuming a planar geometry, we were able to numerically substantiate the experimentalists' observations. We determined that the intended heat source, the oil bath, in fact has two different effects on the system during the various stages of the experiment. Initially, the immersion in the bath keeps the mixture at a temperature that is higher than typical experimental ambient temperatures. Asakura *et al.* reported using temperatures of 45° C to 60° C. While higher than normal room temperature, this range of bath temperatures is low when compared to a typical reaction temperature. Thus, when a reaction front forms, it does so in the center of the tube farthest from the bath. The role of the oil bath becomes that of a heat sink once a thermal front forms. As was reported by Asakura *et al.*, we found that front formation depended on the relationship between tube radius and bath temperature. For a fixed bath temperature, a reaction front is more likely to form in larger test tubes. Defining a clear critical radius as a function of bath temperature, separating initiation and noninitiation conditions, is not possible from the model. However, lower and upper bounds on tube radius that give rise to a reaction front are presented.

REFERENCES

1. A.G. Merzhanov, Self-propagating high-temperature synthesis: Twenty years of search and findings, In *Combustion and Plasma Synthesis of High-Temperature Materials*, (Edited by Z.A. Munir and J.B. Holt) pp. 1–53, VCH, (1990).
2. N.M. Chechilo, R.Ya. Khvilivitsky and N.S. Enikolopyan, The phenomenon of propagation of the polymerization reaction, *Dokl. Phys. Chem.* **204**, 512–513, (1976).
3. N.M. Chechilo and N.S. Enikolopyan, Struction of the polymerization wave front and propagation mechanism of the polymerization reaction, *Dokl. Phys. Chem.* **214**, 174–176, (1974).
4. N.M. Chechilo and N.S. Enikolopyan, Effect of the concentration and nature of the initiators on the propagation process in polymerization, *Dokl. Phys. Chem.* **221**, 391–394, (1975).
5. N.M. Chechilo and N.S. Enikolopyan, Effect of pressure and initial temperature of the reaction mixture during propagation of a polymerization reaction, *Dokl. Phys. Chem.* **230**, 840–843, (1976).
6. P.L. Gusika, The theory of propagation of a polymerization front in a suspension, *Khimicheskaya Fizika* **7**, 988–993, (1982).
7. V.S. Savostyanov, D.A. Kritskaya, A.N. Ponomarev and A.D. Pomogailo, Thermally initiated polymerization of transition metal nitrate acrymide complexes, *J. Polymer Sci. Part A: Polymer Chem.* **32**, 1201–1212, (1994).
8. V.A. Volpert, I.N. Megrabova, S.P. Davtyan and V.P. Begishev, Propagation of caprolactam polymerization wave, *Combustion Explosion Shock Waves* **21**, 441–447, (1985).
9. S.P. Davtyan, P.V. Zhirkov and S.A. Vol'fson, Problems of non-isothermal character in polymerization processes, *Russ. Chem. Reviews* **53**, 150–163, (1984).
10. J.A. Pojman, Traveling fronts of methacrylic polymerization, *J. Amer. Chem. Soc.* **113**, 6284–6286, (1991).
11. J.A. Pojman, A.M. Khan and W. West, Traveling fronts of addition polymerization: A possible new method of materials synthesis, *Polymer Prepr. Amer. Chem. Soc. Div. Polymer Chem.* **33**, 1188–1189, (1992).
12. J.A. Pojman, J. Willis, D. Fortenberry, V. Ilyashenko and A.M. Khan, Factors affecting propagating fronts of addition polymerization: Velocity, front curvature, temperature profile, conversion and molecular weight distribution, *J. Polymer Sci. Part A: Polymer Chem.* **33**, 643–652, (1995).

13. J.A. Pojman, I.P. Nagy and C. Salter, Traveling fronts of addition polymerization with a solid monomer, *J. Amer. Chem. Soc.* **115**, 11044–11045, (1993).
14. A.M. Khan and J.A. Pojman, The use of frontal polymerization in polymer synthesis, *TRIP* **4** (8), 253–257, (1996).
15. J.A. Pojman, V.M. Ilyashenko and A.M. Khan, Free-radical frontal polymerization: Self-propagating thermal reaction waves, *J. Chem. Soc., Faraday Trans.* **92** (16), 2825–2837, (1996).
16. P.M. Goldfeder, V.A. Volpert, V.M. Ilyashenko, A.M. Khan, J.A. Pojman and S.E. Solovyov, Mathematical modeling of free-radical polymerization fronts, *J. Phys. Chem. B* **101**, 3474–3482, (1997).
17. C.A. Spade and V.A. Volpert, On the steady-state approximation in thermal free radical frontal polymerization, *Chemical Engineering Science* **55**, 641–654, (2002).
18. L.R. Ritter, W.E. Olmstead and V.A. Volpert, Initiation of free-radical polymerization waves, *SIAM J. Appl. Math.* (to appear).
19. K. Asakura, E. Nihei, H. Harasawa, A. Ikumo and S. Osanai, Spontaneous frontal polymerization: Propagating front spontaneously generated by locally autoaccelerated free-radical polymerization, In *Nonlinear Dynamics in Polymeric Systems*, ACS Symposium Series No. 869, (Edited by J.A. Pojman and Q. Tran-Cong-Miyata, American Chemical Society, Washington, DC, (2003).
20. G.B. Manelis, L.P. Smirnov and N.I. Peregudov, Nonisothermal kinetics of polymerization processes. Finite cylindrical reactor, *Combustion Explosion Shock Waves* **13**, 389–383, (1977).
21. J. Brandrup and E.H. Immergut, *Polymer Handbook*, Wiley, New York, (1989).